ORIGINAL PAPER

The Tribological Performances of Multilayer Graphite-Like Carbon (GLC) Coatings Sliding Against Polymers for Mechanical Seals in Water Environments

Xiaoyan Guan · Liping Wang

Abstract Graphite-like carbon (GLC) coatings are being increasingly used in mechanical seals, especially under the water-lubricated condition, to improve component durability by providing a low friction coefficient and high wear resistance. We have addressed the friction and wear performances of multilayer Cr/CrN/GLC coatings sliding against polyether–ether–ketone (PEEK), polyimide (PI), and polytetrafluoroethylene (PTFE) in distilled water under various applied loads and sliding speeds using a ring-on-block test rig. Stribeck curves were developed to analyze the water lubrication mechanisms. Start–stop tests were also carried out to evaluate the tribological performances of the coatings. Our results showed that the friction coefficients and wear rates of the polymers decreased with increasing sliding speeds. Compared to the applied load, the sliding speed had a major effect on the friction and wear performance of the polymer. Three coating/polymer tribopairs demonstrated different tribological behaviors, which were attributed to their different molecular structures, the different mechanical properties of the polymers, and the different lubrication mechanisms. The transfer film determined the lubrication mechanism of the three tribopairs and also resulted in the low friction coefficient and wear rate. The initial and steady-state friction coefficient also decreased with increases in the repeated start–stop times. Based on our results, we concluded that the coating/PEEK tribopair presented an excellent tribological performance that we ascribed to the chemical properties of PEEK and the hydrodynamic lubrication regime of the coating/PEEK tribopair at high sliding speeds.

Keywords Graphite-like carbon coatings · Mechanical seals · Tribological performance · Coating/polymer tribopairs · Lubrication mechanism

1 Introduction

Mechanical seals that have been designed to prevent the leakage of liquid or gases in pumps are critical to the safe operation of chemical plants and nuclear power plants, as well as in many aspects of aerospace and petroleum engineering. In general, a soft and a hard material are chosen to be the fixed and rotational rings, respectively, that compose the crucial components of mechanical seals. The criterion of choice for the proper material for the fixed and rotational rings in mechanical seal units is related to the environment (medium) and the operating conditions of the seal (pressure, temperature, and rotational speed). Polyether–ether–ketone (PEEK), polyimide (PI), and polytetrafluoroethylene (PTFE) have excellent properties including a self-lubricating ability, good resistance to chemical erosion, and thermal stability [1–4]. Moreover, the excellent mechanical properties of PEEK owing to its aromatic structure suggests that it is a potential candidate material for mechanical seals in the anti-wear component. Likewise, the high thermal stability of PI and the banded structure and good lubrication properties of PTFE make them potential candidate materials for mechanical seals in the high-temperature and lubrication component,

X. Guan · L. Wang (✉)
State Key Laboratory of Solid Lubrication, Lanzhou Institute of Chemical Physics, , Chinese Academy of Sciences, Lanzhou 730000, People's Republic of China
e-mail: lpwang@licp.cas.cn

X. Guan
Graduate University of Chinese Academy of Sciences, Beijing 100039, People's Republic of China

respectively. In the early stages of mechanical seal development, stainless steel was the material of choice in rotational rings [5]. However, the stainless steel rings were easily corroded and easily worn away in water, weakening the service of the mechanical seals. This was particularly true in the start–stop process and/or conditions involving changes in load/speed: the surfaces of the seals became seriously worn owing to solid-to-solid contact or boundary friction. These deficiencies initiated a search for materials with improved properties, with demand increasing for high-performance mechanical seals able to meet harsher and tougher operating conditions. An alternative approach to enhance the bulk properties of stainless steel is to apply surface engineering and develop coatings to improve the surface performance of the component to satisfy the stringent criteria for mechanical seals under harsh working conditions.

Graphite-like carbon (GLC) coatings, which are characterized by a high hardness, low friction coefficient, high wear resistance, and high chemical inertness [6–10], are the most promising candidates for the improvement of surface properties, especially in terms of tribological performance in humid and water environments. Many researchers have studied GLC properties on different kinds of components to improve their tribological properties. Wang et al. [11] reported that GLC coatings enhanced the tribological performances of Si_3N_4, SiC, and WC under both dry- and water-lubricated conditions. Zeng et al. [12] also stated that the GLC composite coatings demonstrated exceptionally high toughness and high wear resistance on high-speed steel. Moreover, multilayer chromium (Cr)/chromium nitride (CrN)/GLC coatings greatly improved the wear resistance of titanium alloys both under water and in sea water environments [13]. These reports indicate that GLC has the potential to be used as mechanical seals. However, to the best of our knowledge, little information is available on the application of GLC coatings in mechanical seals, especially for multilayer Cr/CrN/GLC coatings coupled with polymers such as PEEK, PI, and PTFE under conditions requiring water lubrication, and the start–stop process for these tribopairs has scarcely been studied.

Based on our results from previously studies, we fabricated multilayer Cr/CrN/GLC coatings on the substrates of stainless steel (Cr18Ni9Ti) rings. We then investigated the tribological behaviors of the coatings sliding against PEEK, PI, and PTFE under different applied loads and sliding speeds, as well as the start–stop processes, in the distilled water-lubricated condition using a ring-on-block test rig. The morphologies of the worn surfaces were also characterized by scanning electron microscopy (SEM) and X-ray photoelectron spectroscopy (XPS).

2 Experimental Details

2.1 Preparation of Multilayer Cr/CrN/GLC Coatings

Multilayer Cr/CrN/GLC coatings were deposited on the substrates of stainless steel rings 1Cr18Ni9Ti. The silicon wafer (p-type 100) was deposited synchronously to provide the typical cross-section of the coatings. Substrates were successively cleaned ultrasonically in acetone and ethanol solutions, each for 30 min, and then placed on a pre-cleaned sample holder for coating. The coatings were deposited using the magnetron sputtering system with twinborn chromium targets and one graphite target between them. Prior to deposition, the substrates were cleaned by Ar ion using pulsed DC bias, and a thin adhesion-promoting Cr layer was first deposited by mid-frequent magnetron sputtering, again with a pulsed DC bias. Nitrogen was then introduced into the chamber to produce the CrN layer. Finally, the top layer of GLC was produced using DC current sputtering with pulsed DC bias. Further details on the deposition of these Cr/CrN/GLC coatings can be found elsewhere [13].

2.2 Coating Characterization

The typical cross-section of the coatings deposited as described above was characterized by field emission SEM (JSM-6701 scanning electron microscope; JEOL, Akishima, Tokyo, Japan). A nanotest600 nanoindenter apparatus (Micro Materials Ltd.) with an indentation depth of 100 nm was employed to evaluate the nanohardness of the Cr/CrN/GLC coating. The adhesion strength of the coating was measured using the scratch test, which was carried out with a diamond indenter (radius 500 μm). The diamond tip was drawn across the Cr/CrN/GLC coating by continuously increasing the normal load by 10 N/min.

2.3 Ring-on-Block Wear Tests

The friction and wear behaviors of the three coating/polymer tribopairs were evaluated by a ring-on-block test rig. The schematic diagram of the tribometer is shown in Fig. 1. The upper specimen (size: 19 × 12 × 12 mm) was composed of a PEEK, PTFE, or PI block; the PEEK and PTFE blocks were obtained commercially from Dongguan Qiwei Industrial Materials Co (Guangdong, China), and the PI blocks were obtained from Shanghai Synthetic Resin Institute (Shanghai, China). It should be noted that PEEK was a composite with some glass fibers fillers. The lower counterpart (size Ø40 × 10 mm) was the stainless steel rings coated by the Cr/CrN/GLC coating. The tests were conducted with the loaded polymers up against the coated

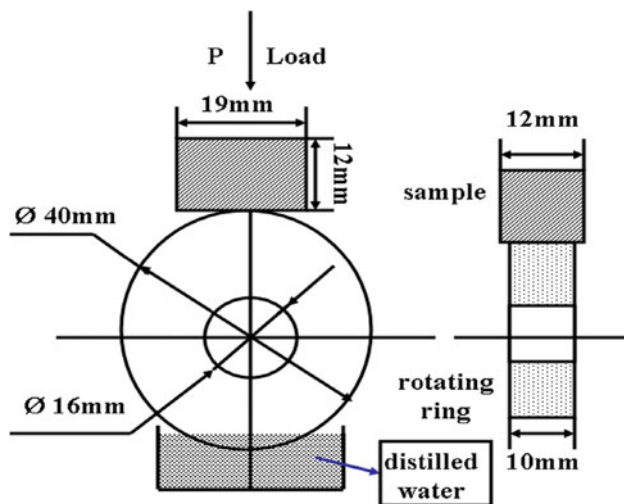Fig. 1 Contact schematic diagram for the frictional couple

Fig. 2 The cross-section of the chromium/chromium nitride/graphite-like carbon (*Cr/CrN/GLC*) coating on silicon wafer

rings with normal applied loads ranging from 80 to 160 N and sliding speeds varying from 0.2 to 0.6 m/s, for a duration of 120 min. Lubrication in the aqueous medium was realized by immersing the lower rings in the distilled water, and the water was taken along the rotation of the rings. The sliding time and friction coefficients were recorded automatically during the tests. The mass loss of each block was measured using an electronic balance (accuracy: 0.01 mg), and the specific wear rate was subsequently calculated according to the following equation:

$$K = \Delta m / (\rho \cdot F_N \cdot L),$$

where Δm corresponded to the mass loss of each polymer block (g) after the test, ρ was the specific gravity of the polymer (g/cm^3), F_N was the applied load (N), and L was the sliding distance (m). Three parallel tests were carried out, and the values were averaged to minimize the error. After the tests, the wear tracks of the rings and counterpart blocks were observed by SEM (JSM-5600). The contact angle of each polymer was measured in order to analyze the frictional behaviors, and XPS was performed on a PHI-5702 multi-functional X-ray photoelectron spectroscope with Al K$_\alpha$ radiation to analyze the chemical status of the typical elements on the worn surfaces of coatings.

3 Results and Discussion

3.1 Characterization of Cr/CrN/GLC Coatings

As the graphite-like characteristic of the as-deposited GLC coatings was not affected by the substrate materials, the GLC coating on the Si wafer was usually employed to investigate the cross-section of the coating [11]. Figure 2 shows the cross-section of the as-deposited coatings on the
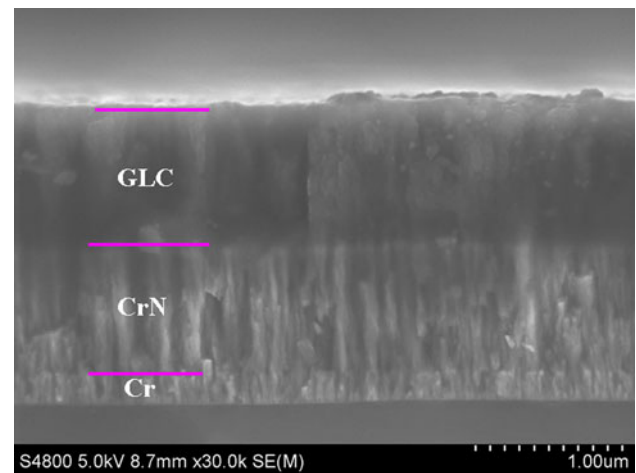
Si wafer. It can be seen that the coating consisted of three layers (Cr, CrN, and GLC) with continuous features and that the intermediate layers were dense and compact. The thickness of the each layer, Cr, CrN, and GLC, was about 0.2, 0.9, and 1.0 μm, respectively. The nanohardness of the Cr/CrN/GLC coating was about 21 GPa, which can be considered as a hard coating. Scratch test results indicated that the critical load for coating delamination was about 32 N.

3.2 Dependence of the Friction Coefficient and Wear Rate on the Applied Load

Figure 3 illustrates the variation in the friction coefficients for the Cr/CrN/GLC coating/polymer (PEEK, PI and PTFE) tribopairs at different applied loads and under the distilled water-lubricated condition. The friction data for each polymer sliding against the uncoated stainless steel ring is also plotted for an applied load of 80 N to serve as a reference. It was evident that the friction coefficients of the coated rings sliding against each of the three polymers were lower than that of the uncoated rings, thereby proving the favorable anti-friction property of the coatings. For the coating/PEEK tribopair (Fig. 3a), the friction coefficients showed little variation and all were relatively stable at approximately 0.1 regardless of the applied loads. However, the friction coefficients of the coating sliding against PI and PTFE first decreased, and then increased with increases in the applied loads (Fig. 3b, c); minimum values were obtained at an applied load of 120 and 100 N, respectively. Compared to the steady-state friction coefficients of the three coating/polymer tribopairs at the same test parameters, PI was the highest (>0.1) followed in decreasing order by PEEK (approx. 0.1) and PTFE (<0.1).
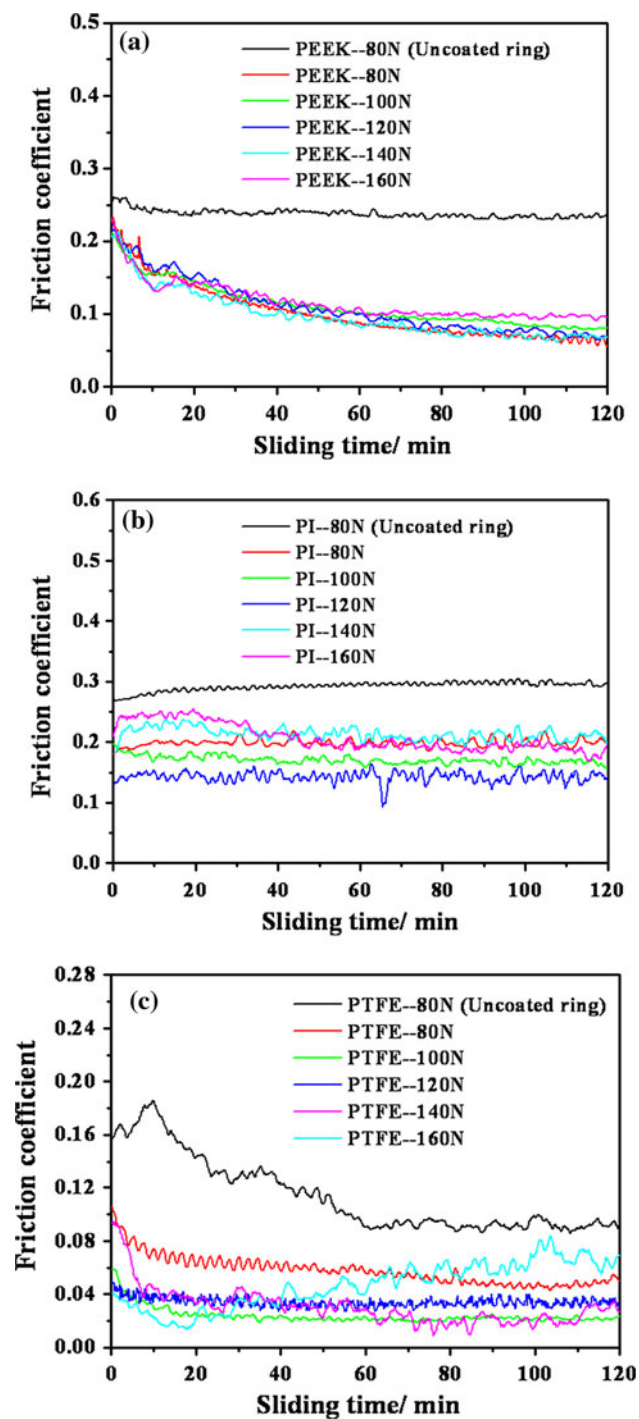
Fig. 3 The curves of friction coefficient vs. sliding time for the coating sliding against each of the three polymers at a sliding speed of 0.2 m/s and at different applied loads in the distilled water-lubricated condition

Table 1 The wear rates of the three polymers at a sliding speed of 0.2 m/s and at different applied loads in the distilled water-lubricated condition

F_N (N)	Wear rate		
	PEEK ($\times 10^{-6}$ mm^3/Nm)	PI ($\times 10^{-5}$ mm^3/Nm)	PTFE ($\times 10^{-4}$ mm^3/Nm)
80–Uncoated ring	68.9	4.69	13.4
80	2.13	2.15	1.96
100	4.99	1.93	2.00
120	3.23	2.07	1.46
140	3.54	3.11	1.51
160	3.53	2.91	1.74

PEEK Polyether–ether–ketone, *PI* polyimide, *PTFE* polytetrafluoro-ethylene, F_N applied load

and PTFE for the respective coating/polymer tribopair decreased by more than one order of magnitude at an applied load of 80 N, while for PI the wear rate decreased by 50 %. At higher loads as well, the wear rates for the coated cases were much lower than those for the non-coated cases. However, for each polymer against the coatings by different applied loads, the wear rates showed slight variation, suggesting that the applied load had only a minor influence on the wear rate. In general, the wear rates for PEEK at any load were approximately an order of magnitude lower than for PI and approximately two orders of magnitude lower than for PTFE.

3.3 Dependence of the Friction Coefficient and Wear Rate on the Sliding Speed

Figure 4 shows the influence of sliding speeds on the friction coefficients for the coating/polymer tribopairs in distilled water. The variation in the friction coefficients for three tribopairs was different with increases in the sliding speed. For the coating/PEEK tribopair, the friction coefficient was stable at around 0.1 at a sliding speed of 0.2 m/s, but it decreased dramatically to approximately 0.04 when the speed increased to 0.3 m/s; there was little variation between the friction coefficient at sliding speeds of 0.3–0.5 m/s. In contrast, the friction coefficient of the coating/PI tribopair fluctuated widely at sliding speeds of 0.3 and 0.4 m/s, respectively, but gradually decreased with increases in sliding speed. For the coating/PTFE tribopair, the friction coefficients gradually decreased to the same value of approximately 0.025 at sliding speeds of 0.2–0.5 m/s and finally dropped to approximately 0.01 at the sliding speed of 0.6 m/s.

Table 2 illustrates the wear rates of the three polymers at different sliding speeds and at an applied load of 100 N in the distilled water-lubricated condition. The wear rates

Table 1 illustrates the wear rates of each of the three polymers against the coatings and stainless steel rings (uncoated rings) as a function of applied load, under the distilled water-lubricated condition. Compared to the uncoated rings/polymers tribopairs, the wear rates of PEEK
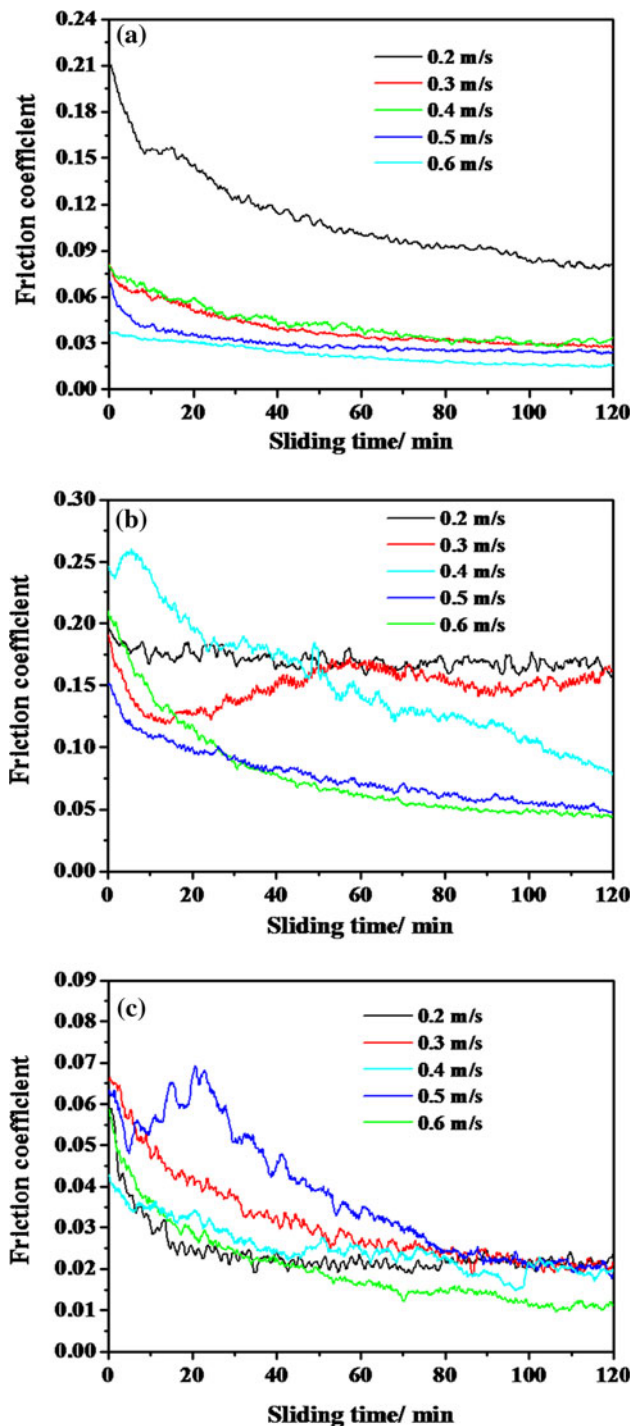
Fig. 4 Friction coefficients for the coatings sliding against three polymers at an applied load of 100 N and at different sliding speeds in the distilled water-lubricated environment: **a** against polyether–ether–ketone (*PEEK*), **b** against polyimide (*PI*), **c** against polytetrafluoroethylene (*PTFE*)

clearly decreased for all polymers with increasing sliding speed and then decreased slightly at higher speeds. PEEK had the lowest wear rate at all sliding speeds.

Table 2 Wear rates of the three polymers at an applied load of 100 N and at different sliding speeds in the distilled water-lubricated condition

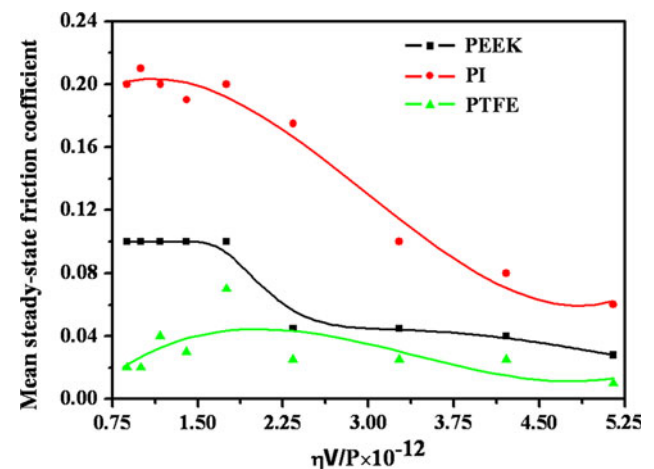| V (m/s)	Wear rate		
	PEEK ($\times 10^{-6}$ mm^3/Nm)	PI ($\times 10^{-5}$ mm^3/Nm)	PTFE ($\times 10^{-4}$ mm^3/Nm)
0.2	4.99	1.93	2.00
0.3	0.88	0.49	1.51
0.4	0.71	0.47	0.55
0.5	0.68	0.39	0.50
0.6	0.40	0.27	0.17

V Sliding speed

Fig. 5 Stribeck curves for the three coating/polymer tribopairs in water

3.4 Water-Lubrication Mechanism of the Coating/ Polymer Tribopairs

To elucidate the water lubrication mechanism of each coating/polymer tribopair, we obtained the mean steady-state friction coefficient for each tribopair (from Fig. 3; Fig. 4), resulting in the construction of a type of Stribeck curve (Fig. 5). From this figure it can be seen that the relationship between the mean steady-state friction coefficient and the Sommerfeld number ηV/P (where η = dynamic viscosity of the lubricant, V = sliding speed, P = mean contact pressure) for each coating/polymer tribopair was different. For the coating/PEEK tribopair, at the lower sliding speed of 0.2 m/s and higher applied load of 160 N, the water lubrication film broke down and solid-to-solid contact was established, resulting in a high friction coefficient (approx. 0.1) and a boundary lubrication (BL) lubrication mechanism. At this lubrication regime, the friction coefficients leveled out and were independent of the Sommerfeld number. With a decrease in applied load, such as an applied load of 80 N, a water lubrication film

would come into existence at the contact interface, resulting in the friction coefficient decreasing rapidly and the water lubrication mechanism changing from BL to mixed lubrication (ML). In addition, when the sliding speed increased to 0.3 m/s and the applied load increased to 100 N, there was no contact between the surfaces, and the friction coefficient tended toward a constant; in this condition, the water lubrication mechanism would change from ML to hydrodynamic lubrication (HL). Thus, the lubrication mechanism changed from BL to ML and then to HL with increasing Sommerfeld number. It was interesting to note that the transition from ML to HL was short and that HL was the dominating lubrication mechanism for the coating/PEEK tribopair. However, for the coating/PI tribopair, at an extremely low sliding speed and high applied load, which was close to the beginning of the curve, the friction coefficient was high at 0.2, which means that the lubrication mechanism was a boundary regime in which the applied load was supported by the contacting surface asperities. With increases in the Sommerfeld number, the friction coefficient gradually decreased owing to the transition from the BL to the ML regime. The Stribeck curve for coating/PI tribopair indicated that the lubrication mechanism changed from BL to ML with increasing Sommerfeld number and that ML was the primary lubrication mechanism. For the coating/PTFE tribopair, the friction coefficient showed little fluctuation with increasing Sommerfeld number. Therefore, it was hard to distinguish the transition in the lubrication mechanism for this tribopair, possibly due to the excellent lubricating properties of PTFE (discussed in following sections).

3.5 Start–Stop Experiments

Solid-to-solid contact occurs during starting and stopping periods, and these may lead to material loss and degradation of the mechanical seal. Therefore, it was important to investigate the tribological performances of the three tribopairs in the start–stop process. We performed the start–stop experiments for three coating/polymer tribopairs for 500 successive times. The duration of each time was 2 min, with a total duration of 1,000 min. Figure 6 presents the schematic diagram of the start–stop process and the corresponding friction coefficients and/or wear tracks for the first, the 250th, and the 500th time. The abscissa represents the cumulative running time, while the ordinate corresponds to the number of repeated times. For the coating/PEEK tribopair (Fig. 6a), the friction coefficient of the first time started at 0.17 and stabilized at around 0.06; when the number of the start–stop times increased to 250, the friction coefficient started at 0.065, then abruptly decreased to around 0.01; at the 500th start–stop time,
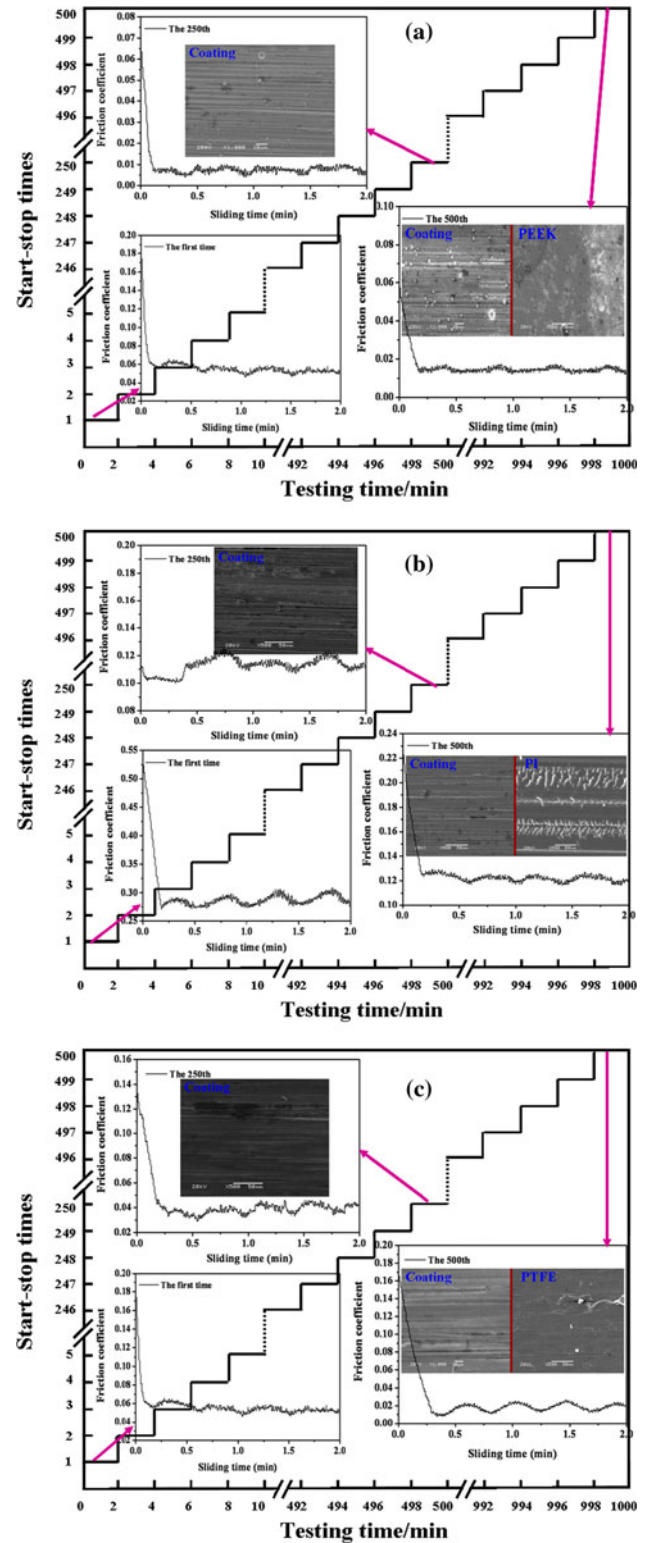

Fig. 6 Schematic diagram of the results of the start–stop tests, the friction coefficients, and/or worn surfaces for the first, 250th, and 500th time for three coating/polymer tribopairs. **a** Coating/PEEK tribopair, **b** coating/PI tribopair, **c** coating/PTFE tribopair. *Abscissa* Total duration, *ordinate* number of running times. The duration of each start–stop test was 2 min

which corresponded to a running time of 1,000 min, the starting friction coefficient was smaller than that at the 250th time. The worn surfaces of the coatings at the 250th and the 500th time showed plough grooves with traces of transfer film. The worn track of the PEEK block slid for 1,000 min was smooth and covered by some fillers. The fillers were able to support the applied load and protect the polymer from severe wear. The steady-state friction coefficient of the coating/PI tribopair showed fluctuations, which became smaller with increases in the number of start–stop times. The worn surface of the coating also showed grooves with traces of transfer film; however, the wear track of the PI block was characterized by plastic deformation and plough grooves. For the coating/PTFE tribopair, the steady-state friction coefficient decreased with increases in the number of start–stop times; however, fluctuation in the steady-state friction coefficient became drastic. The worn surface of the coating was covered by transfer film derived from the PTFE, but the wear track of PTFE was accompanied by plastic deformation and traces of plastic flow. It was interesting to note that there was no delamination or spalling on the worn surface of the coatings, with the exception of the grooves.

### 3.6 Characterization of the Water Contact Angles of Polymers and the Worn Surfaces

The contact angles of three polymers are presented in Fig. 7, which shows the pictures of static contact angles

with a water droplet on the PEEK, PI, and PTFE, respectively. Directly below each picture is the corresponding chemical formula for each polymer. In order to conveniently compare the water contact angles, data were also summarized in the table shown in Fig. 7. It can be seen that PI had the lowest contact angle (below 90°), followed in ascending order by PEEK and PTFE. PI was hydrophilic owing to its imide group, while both PEEK and PTFE were hydrophobic. Concomitantly, the perfluorinated substitution improved the hydrophobicity of PTFE.

Figure 8 illustrates the SEM images of the worn surfaces of coatings and the wear tracks of polymers at test parameters of 160 N and 0.2 m/s. The worn surfaces of the three coatings can be seen to be clearly covered with transfer films and plough grooves of different sizes. However, the worn surfaces of the blocks display different features. The surface of PEEK can be seen to be smooth with some filler dispersion, the PI shows some debris conglobation, while PTFE is characterized by plastic flow trace and plowed grooves parallel to the sliding direction.

Figure 9 shows the XPS spectrums of some typical elements on the worn surfaces of the coatings, in the distilled water-lubricated condition and at an applied load of 160 N and sliding speed of 0.2 m/s. For the worn surface of the coating against PEEK (Fig. 9a), according to Gaussian fitting, the C1s spectrum on the worn surface of coating could be fitted into four components around of 284.9, 286.3, 287.7, and 290.5 eV, respectively. The characteristic peak at 284.9 eV was identified as C–C bonds and

Fig. 7 Contact angles and structural formulas for the three polymers. a PEEK, b PI, c PTFE

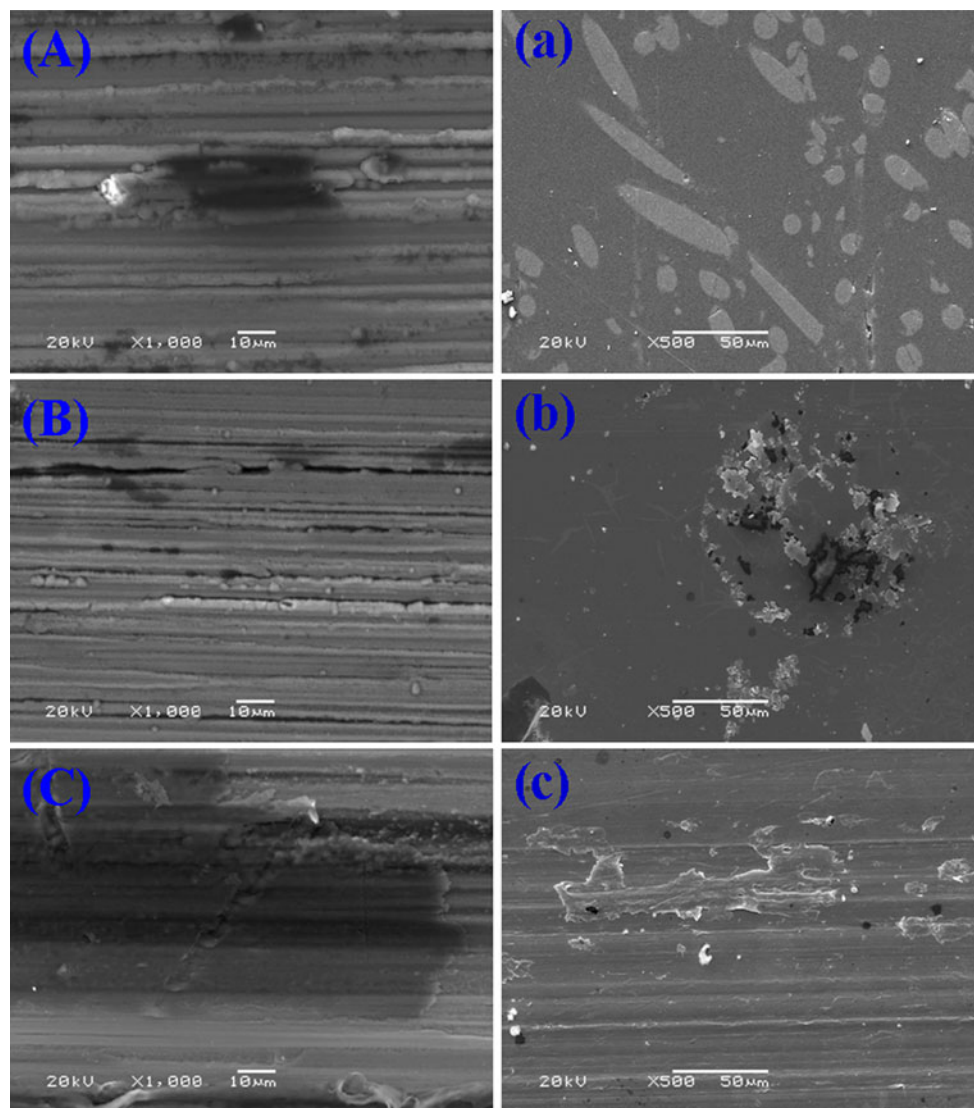|	(a)	(b)	(c)
Contact angle (°)	101.3	81.3	130.5
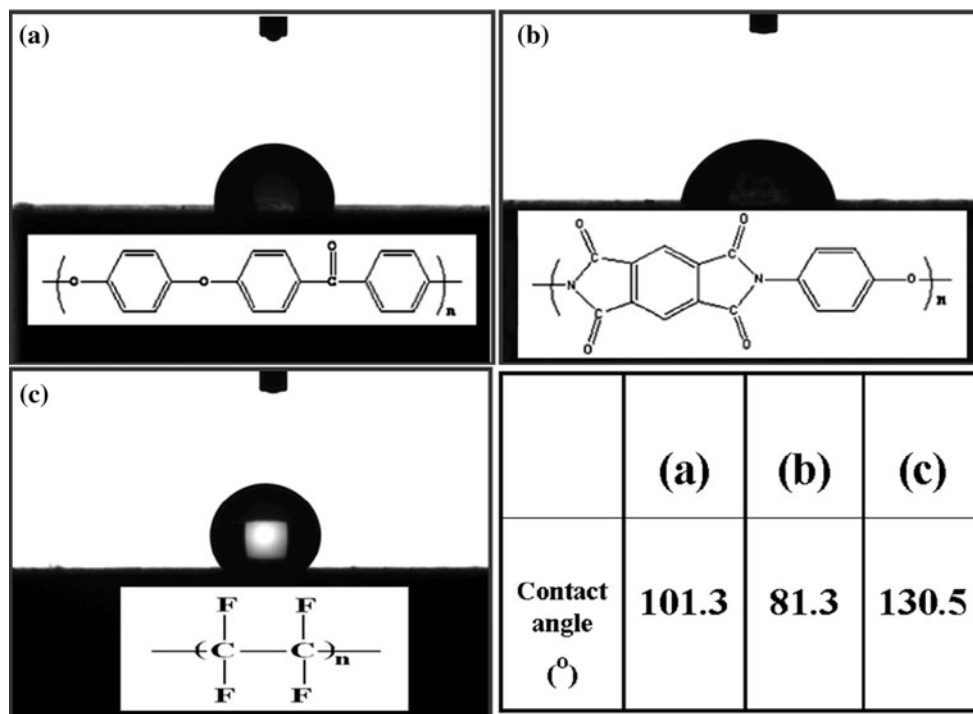
Fig. 8 The scanning electron microscopy morphologies of the worn surfaces of the three coating/polymer tribopairs at 160 N and 0.2 m/s. **A–C** Worn surface of the coating sliding against PEEK (**A**), against PI (**B**), and against PTFE (**C**). **a**, **b**, **c** Evidence of worn tracks of PEEK, PI, and PTFE, respectively

ascribed to the coating; the one around 286.3 eV was ascribed to C–O bonds; the wide peak at 287.7 eV was assigned to C=O bonds. The weak peak at about 291.2 eV was a shake-up satellite due to π–π^* transition and was commonly present in aromatic compounds [14, 15]. The O1s spectra at 532.1 and 534.0 eV were attributed to C=O and C–O groups, respectively. Based on the combined existence of C–O and C=O bonds and the SEM images of the worn surface, we deduced that there was a partial transfer of PEEK to the surface of coatings during the test period. We also deduced that the peak at around 284.9 eV includes aromatic carbon (marked as C-aro in the figure) derived from PEEK. Compared to the coating/PEEK tribopair, the C1 s spectrum for the worn surface of coating

which slid against PI displayed a new peak near 287.1 eV, indicating the formation of a C–N bond on the worn surface (Fig. 9b). The N1s spectrum appearing as a high-intensity peak around 399.7 eV was assigned to a C–N bond, thereby confirming the existence of C–N bonds [16]. Although the O1s presented two peaks at around 532.1 and 534.0 eV, which were similar to those in Fig. 9a, the intensity was inversed, indicating the opposite dominant bonds in the surface. This intensity was consistent with the formulas of polymers shown in Fig. 7. Likewise, the presence of C–N and C=O bonds suggested that there was a transfer of PI to the coating during the frictional test and that aromatic carbon (C-aro) was included in the peak at around 285.0 eV. The C1s spectrum on the worn surface of

Fig. 9 X-ray photoelectron spectroscopy analysis of the worn surfaces of the coatings **a–c** Coating against PEEK (**a**), against PI (**b**), and against PTFE (**c**)
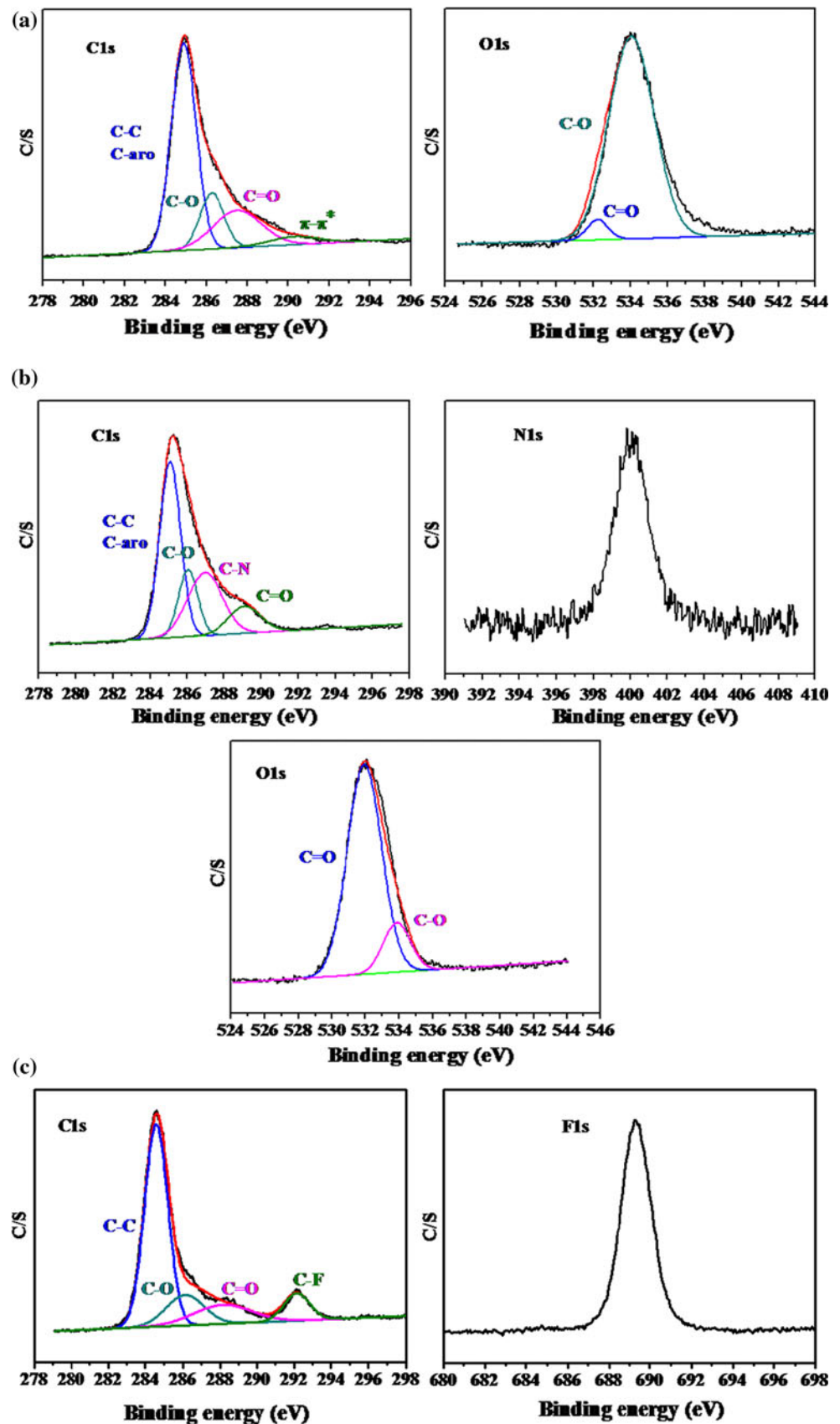
the coating against PTFE also showed four peaks (Fig. 9c), in addition to the two peaks which were similar to the ones mentioned above: the peak at around 284.7 eV was assigned to the C–C bond, and the one near 292.2 eV represented the C–F bond [17]. The high-intensity F1s spectrum at 689.8 eV was associated with the C–F bond, corresponding to the C1s spectrum [17]. On the basis of the SEM images and XPS analysis, it can be confirmed that the transfer film derived from the opposing polymer was formed on each hard worn surface of coating. This result was consistent with other reported studies in which soft materials were transferred to hard materials during the wear process [18].

3.7 Discussion

The tribological property of the solid surface is dependent on the wettability; in other words, the more hydrophobic the surface is, the lower the friction coefficient [19]. Wettability is commonly characterized by contact angle, with a higher contact angle associated with a more hydrophobic surface. This leads to the conclusion that a high contact angle promotes a low friction coefficient. Based on the water contact angles of the three polymers tested in our study (Fig. 7), friction coefficients in order of magnitude of PI > PEEK > PTFE are a reasonable result. Furthermore, the tribological performance of a soft polymer sliding against a hard coating is determined by the transfer ability and build-up of a polymer film [18], and the efficiency in improving the tribological behavior depends on the molecular structure of the polymer [20]. The results of the SEM and XPS analyses confirm that the transfer of the polymer to the opposite coating occurred during the wear process, including the start–stop process. The transfer film on the coating helps avoid direct contact between the polymer specimen and hard coating, decrease the intensely plowing damage, and improve the wear resistance of samples. Without the lubrication of GLC, the friction coefficient and wear rate of the uncoated ring/polymer was relatively high. Similarly, for the start–stop process, the continuous transfer film that was formed with increasing number of repeated start–stop times inhibited the solid-to-solid direct contact and effectively decreased the friction coefficient. Simultaneously, no delamination or spalling could found on the worn surface of the coating, indicating the excellent performance of the Cr/CrN/GLC coating.

The molecular structure and properties of a polymer can also influence tribological behavior. The banded structure of PTFE is easily destroyed due to the low activation energy (7 kcal/mol) of slippage between the crystalline slices, resulting in a low friction coefficient and high wear rate during wear tests [21]. The aromatic ring structure in PEEK and PI restricts chain rotational freedom [22] and

improves stiffness and strength, which is hardly broken down during the wear process; these properties contribute to the high wear resistance of these polymers. However, PI is sensitive to abrasion [23], and any hard surface protrusion increases the deformation component of friction. There was some debris on the wear track of PI, which could increase the difficulty to shear and lead to a high friction coefficient and wear rate. Therefore, we conclude that the tribological performance of the coating/PEEK tribopair was the best among these three tribopairs. In terms of coating sliding against polymers, both the transfer ability and the property of the polymer determined the tribological behavior; however, the property of the polymer was dominant.

The water lubrication mechanism was another factor that was evaluated in terms of its effect on the tribological properties of the tribopairs. The different dependencies between the friction coefficients and the Sommerfeld numbers shown by the three coating/polymer tribopairs (Fig. 5) were related to the lubrication film between the tribopairs after the experiments had been performed in water. It has been reported that the smoother the worn surface, the thicker the average oil film between metal surfaces [24, 25]. By analogy, compared to the worn surface of the three tribopairs, the water film between the coating/PEEK tribopair was the thickest, followed in decreasing order by the coating/PTFE tribopair and the coating/PI tribopair (thinnest). For the coating/PEEK tribopair, at high sliding speed and low applied load, the applied load was supported by the water film, and the lubrication mechanism was mainly HL with little friction and wear. With a decrease in sliding speed or an increase in applied load, the applied load was supported by both a water film and a transfer film, and the lubrication mechanism became ML. At an extremely high applied load or low sliding speed, the water film would be broken down, and the solid-to-solid contact would be established, resulting in severe friction, corresponding to BL. For coating/PI tribopair, the water film was considerably thin, so the applied load would have to be supported by both the water film and the transfer film, possibly contributing to the ML mechanism. However, PTFE could easily form a thin and highly oriented film at the counter surface when the sliding contacts a hard surface, which would lead to a very low friction coefficient [26]. The transfer film decreased the friction coefficient and made it fluctuate slightly irregardless of the applied load or sliding speed. As both the water film and transfer film can decrease the friction coefficient, it was difficult to distinguish whether the interface between the coating and PTFE was filled by water film and/or transfer film. The transition of lubrication mechanism for the coating/PTFE was indistinctive. It is worth noting, however, that the primary mechanism for the

coating/PEEK tribopair was HL, while the coating/PI and coating/PTFE tribopairs was ML or BL. As a result, the former displayed an excellent tribological performance, whereas the latter two tribopairs showed a high friction coefficient and/or high wear rate.

4 Conclusions

The following conclusions can be drawn based on the above results and discussion:

(1) The friction coefficient and wear rate of the tested polymers decreased with an increase in sliding speed. Compared to the applied load, the sliding speed had the more important effect on the friction coefficient and wear rate. The wear rate of PEEK was the lowest among the three polymers and decreased to a magnitude of 10^{-7} mm^3/Nm when the sliding speed was >0.2 m/s.

(2) The transfer film derived from the corresponding polymer on the hard coating contributed to the low friction coefficient and wear rate. Moreover, the water lubrication mechanisms for three coating/polymer tribopairs were different: the coating/PEEK tribopair was mainly in HL, especially at high speed, while the other two were mainly in BL or ML, resulting in high friction or wear.

(3) For the start–stop tests, the start and stable friction coefficients for the three tribopairs decreased with increases in the number of repeated start–stop running times. Moreover, no delamination or spalling could found on the worn surface of coatings, even when the number of repeated times increased to 500.

(4) The coating/PEEK tribopair showed the best tribological performance among the three tribopairs tested. This was ascribed to the better properties of PEEK and the HL mechanism at high sliding speeds. This tribopair provided the superior candidate material for mechanical seals.

References

1. Jia, J., Chen, J., Zhou, H., Hu, L.: Comparative study on tribological behaviors of polyetheretherketone composite reinforced with carbon fiber and polytetrafluoroethylene under water-lubricated and dry-sliding against stainless steel. Tribol. Lett. **17**, 231–238 (2004)
2. Bahadur, S., Polineni, V.K.: Tribological studies of glass fabric reinforced polyamide composites filled with CuO and PTFE. Wear **200**, 95–104 (1996)
3. Xie, W., Pan, W.P., Chuang, K.C.: Thermal characterization of PMR polyimides. Thermochim. Acta **367–368**, 143–153 (2001)
4. Talat, T.: Tribological behaviours of carbon filler polytetrafluoroethylene (PTFE) dry journal bearings. Wear **221**, 61–68 (1998)
5. Mubarok, F., Carrapochano, J.M., Almeida, F.A., Fernandes, A.J.S., Silva, R.F.: Enhanced sealing performance with CVD nanocrystalline diamond films in self-mated mechanical seals. Diamond Relat. Mater. **17**, 1132–1136 (2008)
6. Nakamura, K., Sano, T., Shindo, H.: Frictional property of glass-like carbon heat-treated at 1,000–3,000 °C. Mater. Sci. Eng. B **148**, 242–244 (2008)
7. Field, S.K., Jarratt, M., Teer, D.G.: Tribological properties of graphite-like and diamond-like carbon coatings. Tribol. Int. **37**, 949–956 (2004)
8. Camino, D., Jones, A.H.S., Mercs, D., Teer, D.G.: High performance sputtered carbon coatings for wear resistant application. Vacuum **52**, 125–131 (1999)
9. Yang, S., Camino, D., Jones, A.H.S., Teer, D.G.: Deposition and tribological behaviour of sputtered carbon hard coatings. Surf. Coat. Technol. **124**, 110–116 (2000)
10. Wang, Y.X., Wang, L.P., Wang, S.C., Zhang, G.A., Wood, R.J.K., Xue, Q.J.: Nanocomposite microstructure and environment self-adapted tribological properties of highly hard graphite-like film. Tribol. Lett. **40**, 301–310 (2010)
11. Wang, Y.X., Wang, L.P., Xue, Q.J.: Improvement in the tribological performances of Si3N4, SiC and WC by graphite-like carbon films under dry and water-lubricated sliding conditions. Surf. Coat. Technol. **205**, 2770–2777 (2011)
12. Zeng, X.T., Zhang, S., Ding, X.Z., Teer, D.G.: Comparison of three types of carbon composite coatings with exceptional load-bearing capacity and high wear resistance. Thin Solid Film **420–421**, 366–370 (2002)
13. Guan, X.Y., Lu, Z.B., Wang, L.P.: Achieving high tribological performance of graphite-like carbon coatings on Ti6Al4V in aqueous environments by gradient interface design. Tribol. Lett. **44**, 315–325 (2011)
14. Pireaux, J.J., Riga, J., Caudano, R., Verbist, J.: Electron and ion probes of polymer structure and properties. American Chemical Society, Washington D.C. (1981)
15. Jama, C., Dessaux, O., Goudmand, P., Gengembre, L., Grimblot, J.: Treatment of poly(ether ether ketone) (PEEK) surfaces by remote plasma discharge. XPS investigation of the ageing of plasma-treated PEEK. Surf. Inter. Anal. **18**, 751–756 (1992)
16. Yan, X.B., Xu, T., Chen, G., Yang, S.R., Liu, H.W., Xue, Q.J.: Preparation and characterization of electrochemically deposited carbon nitride films on silicon substrate. J. Phys. D Appl. Phys. **37**, 907–913 (2004)
17. Beamson, G., Briggs, D.: High resolution XPS of organic polymers, the scienta ESCA300 database. Wiley, Chichester (1992)
18. Bahadur, S.: The development of transfer layers and their role in polymer tribology. Wear **245**, 92–99 (2000)
19. Liu, Y.H., Wang, X.K., Luo, J.B., Lu, X.C.: Fabrication and tribological properties of super-hydrophobic surfaces based on porous silicon. Appl. Surf. Sci. **255**, 9340–9348 (2009)
20. Bartenev, G.M., Lavrentev, V.V.: Friction and wear of polymers. Tribology series, vol 6. Elsevier, Amsterdam (1981)
21. Tanaka, K., Uchiyama, Y., Toyooka, S.: The mechanism of wear of polytetrafluoroethylene. Wear **23**, 153–172 (1973)
22. Fusaro, R.L.: Effect of atmosphere and temperature on wear, friction and transfer of polyimide films. ASLE Trans. **21**, 125–133 (1978)
23. Tewari, U.S., Bijwe, J.: Tribological behaviour of polyimides—polyimides: fundamentals and applications, pp 533–583. Marcel Dekker Inc., USA

24. Chow, L.S.H., Cheng, H.S.: The effect of surface roughness on average film thickness between lubricated rollers. J. Lubr. Technol. **1**, 117–124 (1976)
25. Begelinger, A., de Gee, A.W.J.: Failure of thin film lubrication: the effect of running-in on the load carrying capacity of thin-film lubricated concentrated contacts. J. Lubr. Technol. **103**, 203–210 (1981)
26. Lu, X., Wong, K.C., Wong, P.C., Mitchell, K.A.R., Cotter, J., Eadie, D.T.: Surface characterization of polytetrafluoroethrlene (PTFE) transfer films during rolling-sliding tribology tests using X-ray photoelectron spectroscopy. Wear **261**, 1155–1162 (2006)